IEICE TRANS. INF. & SYST., VOL.E87–D, NO.8 AUGUST 2004

PAPER

# Automatic Segmentation of Hepatic Tissue and 3D Volume Analysis of Cirrhosis in Multi-Detector Row CT Scans and MR Imaging

**Xuejun ZHANG**[†a)], **Wenguang LI**[†], *Nonmembers*, **Hiroshi FUJITA**[†,††], *Member*, **Masayuki KANEMATSU**[†††], *Nonmember*, **Takeshi HARA**[††], **Xiangrong ZHOU**[††], *Members*, **Hiroshi KONDO**[†††], *and* **Hiroaki HOSHI**[†††], *Nonmembers*

**SUMMARY** The enlargement of the left lobe of the liver and the shrinkage of the right lobe are helpful signs at MR imaging in diagnosis of cirrhosis of the liver. To investigate whether the volume ratio of left-to-whole (LTW) is effective to differentiate cirrhosis from a normal liver, we developed an automatic algorithm for three-dimensional (3D) segmentation and volume calculation of the liver region in multi-detector row CT scans and MR imaging. From one manually selected slice that contains a large liver area, two edge operators are applied to obtain the initial liver area, from which the mean gray value is calculated as threshold value in order to eliminate the connected organs or tissues. The final contour is re-confirmed by using thresholding technique. The liver region in the next slice is generated by referring to the result from the last slice. After continuous procedure of this segmentation on each slice, the 3D liver is reconstructed from all the extracted slices and the surface image can be displayed from different view points by using the volume rendering technique. The liver is then separated into the left and the right lobe by drawing an inter-segmental plane manually, and the volume in each part is calculated slice by slice. The degree of cirrhosis can be defined as the ratio of volume in these two lobes. Four cases including normal and cirrhotic liver with MR and CT slices are used for 3D segmentation and visualization. The volume ratio of LTW was relatively higher in cirrhosis than in the normal cases in both MR and CT cases. The average error rate on liver segmentation was within 5.6% after employing in 30 MR cases. These results demonstrate that the performance in our 3D segmentation was satisfied and the LTW ratio may be effective to differentiate cirrhosis.

***key words:*** *MR imaging, liver, cirrhosis, image segmentation, contour detection*

## 1. Introduction

Cirrhosis of the liver is a late stage of progressive liver disease defined as structural distortion of entire liver by fibrosis and parenchymal nodules. Early diagnosis is critical in cirrhosis to establish the cause of the disease and to determine the amount of existing liver damage. Although there is no effective treatment for decompensate or advanced cirrhosis, interferon therapy is sometimes beneficial for early cirrhosis associated with viral hepatitis [1]. Therefore, the early detection of cirrhosis may help determine proper treatment in patients with this disease. The diagnosis of cirrhosis is carried out by physical inspections, serological tests, radiologic imaging (computed tomography [CT], magnetic resonance imaging [MRI], scintigraphy, or ultrasonography), liver biopsy, or a combination. As the liver parenchyma regenerate after hepatocyte necrosis, fibrosis of a variety of degree develops throughout the liver and cause gross distortion in configuration to the liver [2], [3]. Morphologic analysis is regarded as an important and useful tool to differentiate cirrhosis from a normal liver. Many efforts have been done by investigating hepatic morphologic changes on imaging, such as CT, MRI and ultrasonography. Changes in liver volume predicts the prognosis of patients with cirrhosis, but the measurement needs quantitative, reproducible methods, that can be achieved only by imaging techniques. Classically, physical examinations performed by percussion and palpation showed that the difference between actual liver volume and the value predicted by liver span was large [4]. Sahin et al. [5] estimated the liver volume by the Cavalieri principle using MRI. McNeal et al. [6] investigated a method for measuring the volumes of human livers in vivo from MRI and subsequently displaying these livers in three dimensions. These results indicated that both processing methods had a high degree of volume-measuring accuracy. However, cirrhotic livers only slightly reduce in size compared with healthy livers when enlargement of the left hepatic lobe and shrinkage of the right hepatic lobe take place in cirrhosis. The whole liver volume could not provide significant value in the diagnosis of cirrhosis. Awaya et al. [7] measured caudate-right lobe (C/RL) ratio with use of the right portal vein to overcome the above mentioned problem. The diagnostic accuracy is not yet satisfied due to the result only from one 2D MR image. In this paper, we propose a novel method to quantitatively calculate the degree of cirrhosis from extracted three-dimensional (3D) liver based on volume analysis.

A number of groups have developed techniques for the purpose of segmentation of the abdominal organs on CT images, but there are no reports on MR images, as far as we know. Bae et al. [8] used a threshoding method to segment the liver in living-donor abdominal CT images. In this method, a gray-level threshold was determined from the histogram, therefore the segmentation would be affected by other connected organs or tissues with the overlap density. Park et al. [9] presented their method to construct a probabilistic atlas of an abdomen consisting of four organs. By registering each organ separately, better overall accuracy

Manuscript received August 25, 2003.
Manuscript revised January 30, 2004.

[†]The authors are with the Electronics and Information Systems Engineering Division, Graduate School of Engineering, Gifu University, Gifu-shi, 501–1193 Japan.
[††]The authors are with the Department of Intelligent Image Information, Division of Regeneration and Advanced Medical Sciences, Graduate School of Medicine, Gifu University, Gifu-shi, 501–1194 Japan.
[†††]The authors are with the Department of Radiology, Gifu University School of Medicine, Gifu-shi, 501–1194 Japan.
a) E-mail: zhang@fjt.info.gifu-u.ac.jp

was obtained even with noncontrast CT scans. However, manually putting 17 control points and selecting reference patient make it impractical in our cirrhotic study, since the morphology change in cirrhosis is very large and the atlas is hard to be constructed properly. Masumoto et al. [10] developed their method by using two different phase images on the liver region. The liver was enhanced effectively to raise the accuracy of segmentation, but meanwhile increased the complicacy of routine. Furthermore, this method could not be extended to the MR imaging.

In this paper, we propose an automatic method of finding the initial liver contour and calculating the gray-level threshold value to reconfirm the final region.

## 2. Method

### 2.1 Image Data Collection

Thirty patients underwent MR imaging with a 1.5-T superconducting magnet (Signa Horizon; GE Medical Systems, Milwaukee, Wis.). The gadolinium-enhanced gradient-recalled-echo portal venous images were obtained using a phased-array body multi-coil with the following settings: echo time (TE) 1.6 ms, repetition time (TR) 150 ms, flip angle 90°, matrix 512 × 512, 26-second breath-hold acquisition. Images were obtained after an antecubital intravenous bolus injection of 0.1 mmol/kg of gadopentetate dimeglumine (Gd-DTPA) (Magnevist; Schering AG, Berlin, Germany) followed by 15 ml of sterile saline solution flushed. The scan timing was 60 seconds after initiating the contrast injection. The presence of cirrhosis was confirmed by two experienced radiologist (H.K., M.K.) in the 30 patients including 15 patients with cirrhosis and 15 without. From all of the MR images in each case, we selected one gadolinium-enhanced late-phase MR image depicting the largest liver area. The liver contours were manually traced by the radiologists for the establishment of standard-of-reference liver contours for programming. The 30 cases (each only contains one 2D slice) were selected for segmenting liver region and 4 cases including normal and cirrhosis liver with multi-slices both in MR and CT images were used for 3D segmentation and visualization. The CT images were acquired using a helical CT scanner (LightSpeed Ultra; GE Medical Systems), with parameters: tube voltage 120 kV, tube current 300 mA, slice thickness 1.25 mm and exposure time 554 ms.

### 2.2 The Liver Structure and Its Segments

The liver is one of the biggest organs in human body. Because of its special supply system by two types of veins (hepatic and portal veins), the couinaud classification is widely accepted as a criterion that divides the liver into 8 independent segments for the purpose of resections. Figure 1 (a) shows that the right hepatic vein (RHV), the middle hepatic vein (MHV), the left hepatic vein (LHV) and

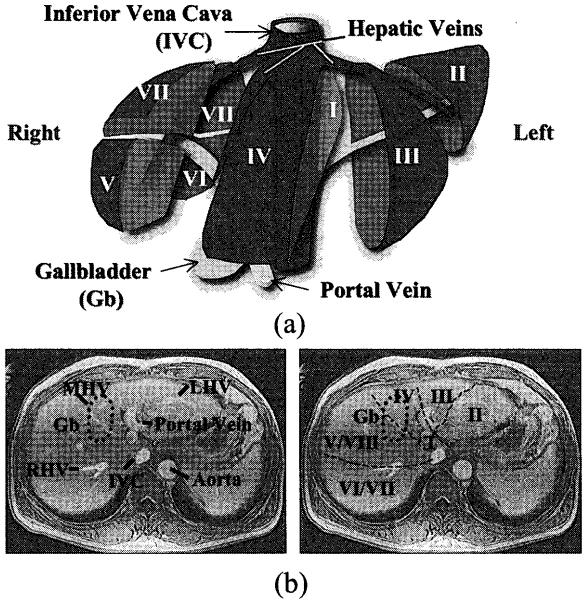


**Fig. 1** An anatomical figure illustrates (a) the couinaud liver segments, and (b) its MR images are shown below.

the portal vein (PV) with gallbladder plane provide the references for separating the liver segments. From the MR images shown in Fig. 1 (b), we can notice that the inferior vena cava (IVC) is passed through the segment I (the caudate lobe) near aorta, and gallbladder always locates in segment IV (the quadrate lobe). These anatomical knowledge may help us to extract the liver region and separate it for cirrhosis calculation. In our study, we define the segment II and segment III as the left hepatic lobe. Other segments belong to the right hepatic lobe, even though the segment IV is regarded as medial left lobe by anatomists.

### 2.3 Segmentation of Liver Region

We developed an algorithm for segmentation of the liver region from other organs and tissues on the portal venous phase images. Two edge operators are applied to obtain the initial liver area, from which the mean gray value is calculated as threshold value. The final contour is re-detected by using thresholding technique. As shown in Fig. 2, our method consists of three main steps: I. Preprocessing step to diminish and smooth the original image; II. Extracting step to obtain the initial liver contour by edge operators; III. Re-detecting step to confirm the final liver region.

(a) Preprocessing

The purpose of the preprocessing step is to unify the MR images into a standard condition, in which the position and size of the liver area are relatively the same, as well as some reference objects like aorta. The contour of abdominal body is firstly extracted by thresholding method, as this part is obviously brighter than its black background. The characters and numbers on MR images can be eliminated completely and the ROIs only contain maximal size of abdominal contents. Secondly, average smoothing with 4 × 4 neighbors

is applied for reducing the effect of noise, meanwhile enlarging the width of liver edge. Finally, to avoid too many labeling numbers and missed detection of the aorta and the liver location, the size of image is limited to a range around 200 to 280 pixels width by diminishing with a proper ratio according to the size of ROI.

(b) Edge detection by combination of Sobel and LOG filters
When applying the thresholding technique to separate the object from background, it is difficult to: 1) determine a proper threshold value and 2) distinguish the connected organs or tissues that sometimes show relatively high or low intensities to the liver region, for example, the kidney or the stomach. Human can easily recognize the liver from MR images not only because of its big size, but also its different intensity from the other components, that is especially obvious at the edge of a liver. Therefore, our strategy is to first focus on the edge information. Figure 3 (a) shows an MR image $I(x, y)$ with a cirrhotic liver. We should notice that the liver region consists of the hepatic tissues and white vessels.

If a pixel falls on the boundary of an object in an image, then its neighborhood will be a zone of gray-level transition.

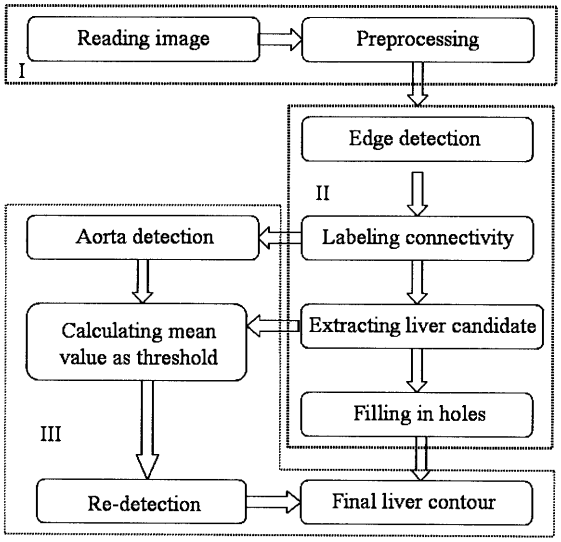


**Fig. 2** Overall flowchart of segmentation in a slice containing biggest liver region.

Our first edge detector is the Sobel filter, which is based upon convolution with an eight-directional $3 \times 3$ derivative mask as shown in Fig. 4. The output of each pixel is to select one of the largest values among 8 directions after applying the Sobel masks. The benefit of this filter is that we can obtain strong edges at any direction since the liver contour is closed. The output shown in Fig. 3 (b) is an edge magnitude image.

The Laplacian-of-Gaussian (LOG) operator, which has been suggested by Marr and Hildreth [11] whilst studying the human visual, is regarded as one of the best edge detectors. By combining the Sobel and LOG filters, we can extract the subtle edges that should be missed by each of the individual methods (in order to make an obvious effect, Fig. 5 uses an artificial pattern instead of a real liver). The Laplacian is often applied to an image that has first been smoothed with a Gaussian smoothing filter in order to reduce its sensitivity to noise. The image $I(x, y)$ is first smoothed with Gaussian filter, that its 2-D response function can be given by

$$G(x, y) = \frac{1}{2\pi\delta^2} \exp\left(-\frac{x^2 + y^2}{2\delta^2}\right). \tag{1}$$

Then sharpen it with a Laplacian differential operator:

$$\begin{aligned} f(x, y) &= \nabla^2\{G(x, y) \times I(x, y)\} \\ &= \nabla^2\{G(x, y)\} \times I(x, y) \\ &= \frac{1}{2\pi\delta^4}\left[\left(\frac{x^2+y^2}{\delta^2} - 2\right)\exp\left(-\frac{x^2+y^2}{2\delta^2}\right)\right] \times I(x, y). \end{aligned} \tag{2}$$

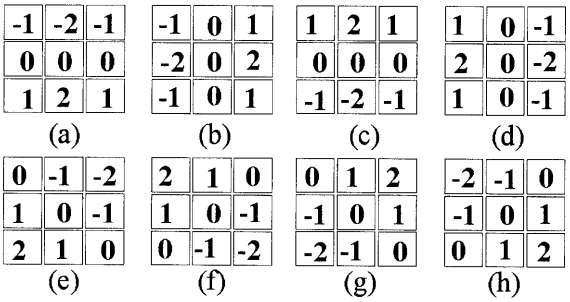


**Fig. 4** (a)–(h) represent eight-directional $3 \times 3$ derivative masks of Sobel filter.

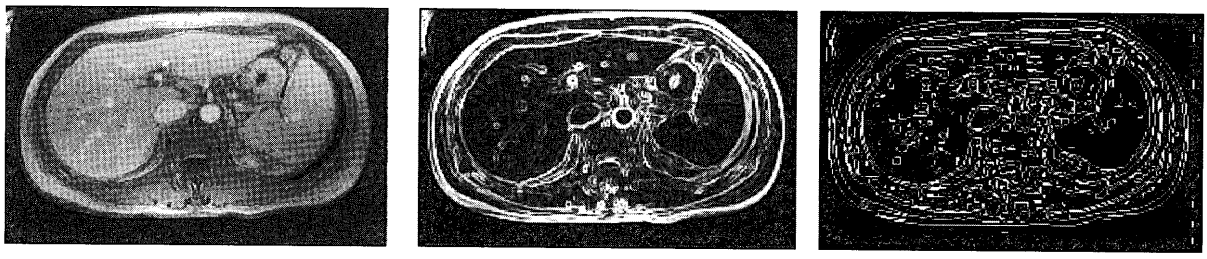

(a) (b) (c)

**Fig. 3** (a) Preprocessed image $I(x, y)$ derived by smoothing and diminishing from original MR image. (b) Magnitude image by using Sobel filter. (c) Binary image after processing (b) by LOG algorithm.

The zero crossing detector looks for places in the Laplacian of an image where the value of the Laplacian passes through zero-points where the Laplacian changes sign. Such points often occur at edges in images. Zero crossings always lie on the closed contours, and so the output from the zero crossing detector is usually a binary image with single pixel thickness lines showing the positions of the zero crossing points.

Figure 3 (c) shows the output image after implementing LOG operator to the magnitude image derived from Sobel filter (b), where one edge line on Sobel image corresponds to two parallel edge lines on LOG image. All the connected taggings below 3 points are eliminated as noise. After edge detection, the inside hepatic tissues are turned into black and only remains a closed contour along liver surface as shown in Fig. 3 (c).

The main idea of picking up liver region is to describe a closed contour that can noose the black liver region. Therefore, it will cause troubles if this boundary is not closed. Thickening each point can be helpful to reduce such problem [Fig. 6 (a)]. In our program, 4 neighbor points are expanded if a point is white in Fig. 3 (c).

(c) Selecting the initial liver region

The aorta is an important reference coordinate for its position that always locates on the under-right side of liver near the caudate lobe, and it indicates high intensity with a circle shape. The aorta can be found by the following 3 features: circularity, area and position. All centroids of connectivity are calculated from labels, and circularity $e$ can be defined as $S2/S1$, where $S1$ is the area of one label, while $S2$ is the common area of $S1$ and a circle with the same area as $S1$ on the centroid of this label. The size of aorta is often between 30–60 pixels according to the image size in our experiment, and its position locates on nearby middle of abdominal body. Therefore, if labeled connectivity satisfied with the condition of area and position features, we can select two candidates with highest $e$ value identified with the aorta and the IVC. Since the aorta always locates on the right side of the IVC, our program can robustly select the aorta referring to this anatomical criterion. The liver and the background region have biggest area in all the connected white pixels, but the position of these two areas is quite different. The liver candidate could be found out among all the labeled white components by maximum area except for the background and by referring to information of location (on the left side of MRI and upper-left side of the aorta). Figure 6 (b) illustrates a selected liver structure.

The extracted liver area only contains hepatic tissues without other organ structures or vessels inside that may change the value of calculating liver intensity if being included. This is due to the fact that edge detector only concerns about different intensity between them, no matter what the explicit number is. The conventional thresholding technique is hard to solve this problem because there are different kinds of non-hepatic structures that should be darker or brighter than liver area. We can calculate the mean intensity of the liver $G_{avr}$ by:

$$G_{avr} = \frac{1}{n} \sum_{(x,y)\in R} I(x,y), \tag{3}$$

where $R$ is the specified liver region shown in Fig. 6 (b), and $n$ is the number of pixels within the region.

(d) Re-detection by thresholding technique

If the contour is not completely closed, undesired parts will connect to the liver region [Fig. 6 (b)]. The main reason of this occasion is that the edge between the liver and tissues is indistinct. However, in many cases the intensity between these two structures is various, that makes it possible to use thresholding technique for component decomposition. Holes inside the initial area are filled in so as to make a mask of the initial liver region $M_{ini}(x,y)$ as shown in Fig. 6 (c),

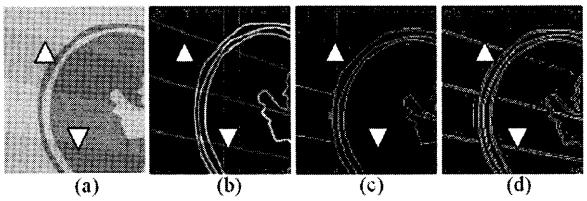


**Fig. 5** An simulation image (a) has a slight block (arrows) crossing the image pattern. Results derived from applying Sobel filter only (b), LOG filter only (c), and Sobel+LOG filter (d) indicate that combination of two filters may extract very subtle edge rather than use them individually.


**Fig. 6** Thickened image (a) enlarges every detected edge to make liver contour closed as much as possible. Liver structure (b) can be selected from all the labeled black area, in which the inside holes are filled to make the mask of initial liver (c). After reading gray values from preprocessed image in Fig. 2 (a), restricted contour image (d) defined as $I'(x,y)$ is derived to be calculated mean gray value as the threshold value in re-detection step.

from which we may obtain a contour restricted gray-value image $I'(x,y) = I(x,y) \times M_{ini}(x,y)$ as shown in Fig. 6 (d). Although the connected parts have some affection on calculating the average value of liver, considering of the large area of liver, these affections may be ignored.

Livers on MR image often appear to be heterogeneous in different part. The intensities near the abdominal surface where the coins are placed indicate high value compared with those inside the deep human body. Thus on the 2-D MR image, the liver shows brighter on the upper side than lower side. Therefore, we apply two threshold values $G_{up}$ and $G_{low}$ on $I(x,y)$ to reconfirm the upper and lower side liver. The average standard deviation of a liver region is within the gray value of 10 in a pre-processed 8-bit image, and the difference of intensity between the upper and the lower side of liver is around 20. In our experiment, we empirically select $G_{up} = G_{avr} - 10$ and $G_{low} = G_{avr} - 30$, respectively. Because of the high threshold value, upper side re-detection may erode the different surrounding connections without affecting on the lower side liver. After labeling the binary image gained by threshold $G_{up}$, the liver is picked up as mask $M_{up}(x,y)$ and compare with the former mask $M_{ini}(x,y)$, a new upper side mask can be given by $M'_{up}(x,y) = M_{up}(x,y) \cap M_{ini}(x,y)$. Using the lower threshold $G_{low}$ may cause undesired reconnection on the upper side, our method of re-detection the lower side liver is limited in the region of under the line $L_s$. As the aorta always closes to and parallels with the IVC passed through liver segment I, drawing a line between the center of aorta $(x_{aorta}, y_{aorta})$ and the minimum coordinate of the abdominal wall can robustly separate the liver region near the coil from the deep parts. $L_s$ can be formulated by $y = (y_{aorta}/x_{aorta})x$. A reconfirmed lower side mask can be expressed as $M'_{low}(x,y) = M_{low}(x,y) \cap M_{ini}(x,y)$. The final liver mask is calculated from:

$$M_{liver}(x,y) = M'_{up}(x,y) + M'_{low}(x,y) + M_{aorta}(x,y), \quad (4)$$

where $M_{aorta}(x,y)$ is the mask re-detected from area between aorta and the bottom of upper side as shown in Fig. 7. The final liver contour is shown in Fig. 8.

Not like MR imaging, the intensity distribution of a liver region in CT images is homogenous, therefore in the re-detection step, only one threshold value $G_{avr}$ is applied to re-confirming the final contour in CT images.

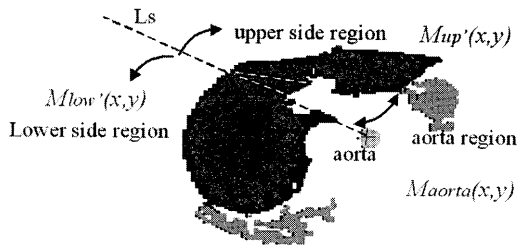


**Fig. 7** Re-detection of upper and lower side of liver. Initial liver [Fig. 6 (a)] is re-detected by thresholding method. The black region is the confirmed precise liver, and the gray parts are eliminated connections.

(e) Evaluation of the performance

To evaluate the segmentation performance, the gold standards of the liver contour were drawn by an experienced radiologist as shown in Fig. 9 (a). Area within this contour was calculated as $A_{gold}$. By comparing with the area of detected liver region $A_{det}$ shown in Fig. 9 (b), error can be defined as the ratio of different liver area $A_{err}$ between reference and detection divided by the reference liver area. $A_{err}$ can be calculated by XOR operation on the masks of gold standard and the detected liver region: $A_{err} = A_{gold} \oplus A_{det}$.

### 2.4 3D Segmentation and Visualization

The above algorithm is modified to be able to extract a small liver region by using the result from the last slice. Because the interval of MR slices is always over 5 mm, the liver changes its shape greatly on its nearby slices. Therefore our method is based on 2D rather than 3D image processing techniques. 3D MR image is constructed from about 25 slices and the surface image can be displayed from the different view points by using the surface rendering or volume rendering technique. Figure 10 (a) and (b) show a normal liver and a cirrhosis liver, respectively. Also this method may extend to extract the liver region or other organs on CT images as shown in Fig. 10 (c) and Fig. 10 (d).

### 2.5 Calculating the Degree of Cirrhosis

Lobar or segmental changes of hepatic morphology are common appearances seen in advanced cirrhosis. These appearances typically include atrophy of the right hepatic lobe and the left medial segment and enlargement of the caudate lobe and the left lateral segment. The ratio between the transverse width of the caudate lobe and the right lobe can be used for differentiating normal from advanced cirrhotic livers [7]. However, this ratio does not help to identify the presence or absence of early cirrhosis. Furthermore, the liver often changes its shape in different sleeping postures, and the ratio may be changed in different inspection time only using one 2D slice. 3D imaging can solve this problem, since volume is the same no matter how the shape is varied. The liver is separated into left and right lobe by draw-

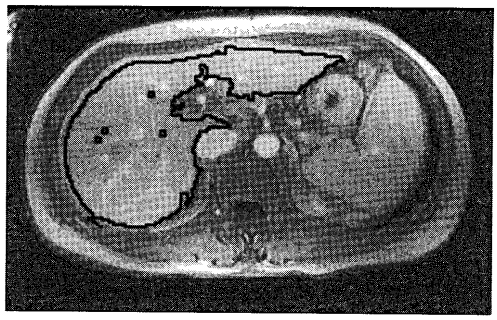

**Fig. 8** The black line described is the extracted liver contour, which seems to be smaller than the real liver because of the absent pixels of thickened edge when selecting the initial liver structure.

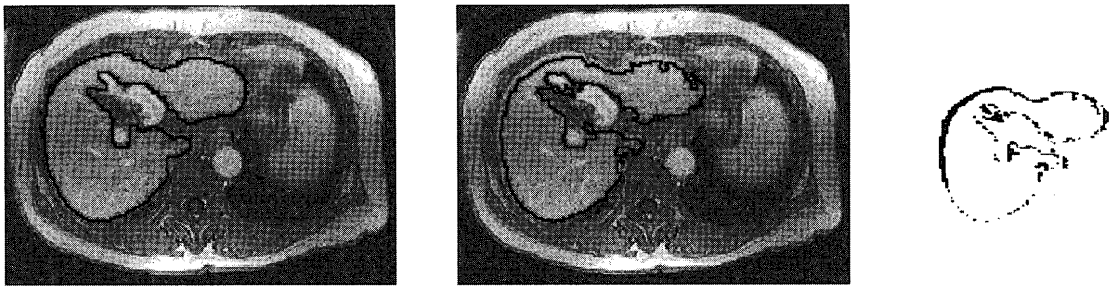

(a) (b) (c)

**Fig. 9** An example of cirrhosis case image with a liver contour drawn by an experienced radiologist in (a) as the reference liver contour. (b) is the result of liver contour drawn by our segmentation program. Error image (c) shows the difference between detected and desired images.

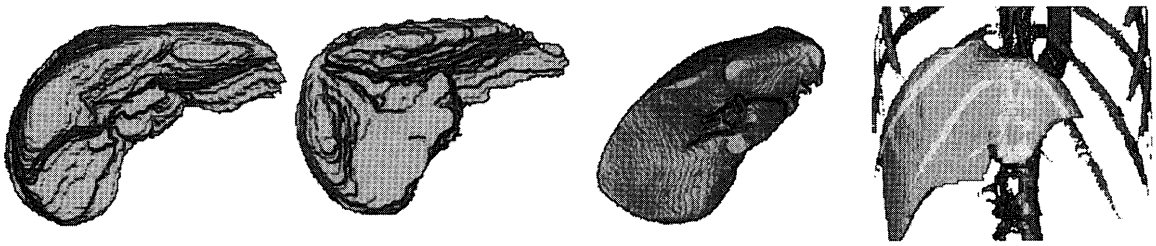

(a) (b) (c) (d)

**Fig. 10** Livers constructed by extracted 2D liver regions from MR images with a slice interval of 5 mm indicate that the volume ratios between left and right side of liver are different in a normal case (a) and cirrhosis case (b). (c) Livers constructed from CT images with a slice interval of 1.25 mm. (d) Liver, aorta, costa and spine are extracted from CT images by using our same edge detection based method developed for MR images.

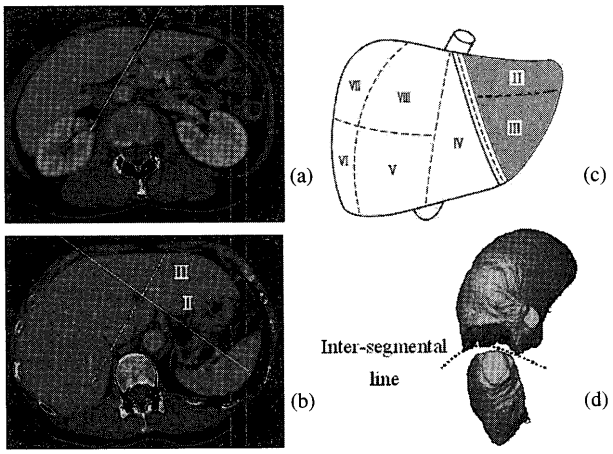


**Fig. 11** Inter-segmental line (white) can be drawn by two lines in (a) and (b) slices manually. (c) Segments II and III are mainly included in the area that separated by the two lines. (d) shows the segmented result in 3D.

ing an inter-segmental line that is decided by two straight line in Fig. 11 (a) and (b), respectively. In our experiment, selecting these two slices is manually feasible because our program does not contain the function on liver shape analysis, and the classification of the liver segments needs to extract the hepatic and portal veins accurately. To draw the line in Fig. 11 (a), a slice with segment II obviously separated from the right side of the liver is selected. Another slice is chosen if the bifurcation of the main portal vein can be seen as in Fig. 11 (b). These procedures are relatively easier jobs by doctors than computer, and the consistency of drawing the inter-segmental line by different radiologists is very high. The inter-segmental line mainly divided liver region into segments II and III and other parts as shown in Fig. 11 (c) and a real result in this case is displayed by 3D image as in Fig. 11 (d). The volume ($V$) in each part is calculated slice by slice. The degree of cirrhosis is defined as ratio of LTW = $Vleft/(Vright + Vleft)$.

### 2.6 Software and Hardware of Our Scheme

We implement a prototype tool using Visual C++ within WindowsXP running on a PC (Pentium M 1 GHz with 512 MB RAM). The graphic user interface of our software is consists of an image window, the folder and file boxes, toolbox and information windows as shown in Fig. 12 (a). The current vision of our program supports DICOM, BMP or raw data file formats. Image files can be selected and displayed just by clicking the file name from the folder and the file boxes. The radiologists are able to zoom the image and interactively change the contrast and brightness of the displayed images according to their preference. Once a case is confirmed and a slice with largest liver region is selected, the radiologist may press the "segmentation" button to wait the result of liver coming out. The processing time in one slice is about 3 to 5 seconds. In a MR case with a slice interval of

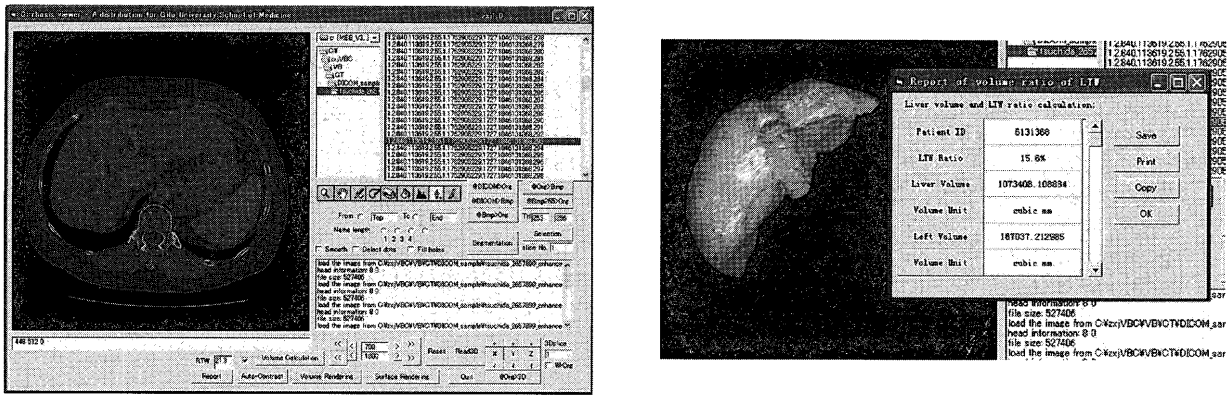

(a) (b)

**Fig. 12** (a) is the user interface that enables doctors to segment liver region; calculate liver area; view slices sequentially; edit pictures or make inter-segmental line. (b) shows of a 3D liver visualized by surface rendering and its results containing LTW ratio in a message box.

5 mm, segmentation of the liver region averagely costs 54 to 90 seconds. In a CT case with a slice interval of 1.25 mm, the average time is around 2.5 times than in MR. The surface rendering and volume rendering techniques are used in the 3D visualization preference study. Construction of a 3D surface image often takes 10 to 20 seconds before the user may view the liver freely by moving the mouse. Since the radiologists can only view 2D images by traditional MR and CT device, our software may provide additional 3D information to facilitate their daily interpretation. For example, the whole shape and the volume of a liver or even roughness of a liver surface would be helpful to their cirrhosis analysis. The volumes of liver or liver segments can only be measured from three-dimensional images, as the classical image editing tools are time request and impossible to be utilized in a clinical routine. To calculate the volume ratio of LTW, the program is asked the user to use the "draw" function button from the toolbox to put two inter-segmental lines following the instruction shown in Fig. 11 (a) and (b). The final result will be informed in an information message box and displayed on the image window as shown in Fig. 12 (b).

## 3. Result and Discussion

Table 1 illustrates the result of a MR case in Fig. 3. Figure 3 (a) was derived from smoothing and diminishing the original image. After employing the Sobel and the LOG filters, the initial liver structure shown in Fig. 6 (b) was selected from the dark labelings on the thickened image Fig. 6 (a). Two connected organ and tissues were located in the upper and the lower side of liver, respectively. The average value of the liver tissue $G_{avg}$ was calculated by adding all the pixel values if the corresponding pixel was black on Fig. 6 (b). In this case of 8-bit image, the $G_{avg}$ is 154. The first mask of liver area [Fig. 6 (c)] was made by filling the holes in Fig. 6 (b), then the program read the gray-value from Fig. 3 (a) according to the mask and gave a contour restricted image [Fig. 6 (d)], in which three regions were defined: the upper side, the lower side and the aorta

**Table 1** Result of an MR case in Fig. 3.

| Item | Content | Unit |
|---|---|---|
| Image depth | 8 | bits |
| Image Size | 512X512 | pixels |
| Average gray value of initial liver ($G_{avg}$) | 154 | pixel values |
| Gold area of liver $A_{gold}$ | 5121 | pixels |
| Error pixels | 502 | points |
| Error rate | 9.8 | % |
| Processing time | 3 | seconds |

area [Fig. 7]. The re-detection process was undertaken on each of these regions. An area that was reconfirmed as part of liver will be turn into black, and the whole liver region was the sum of the three re-detection components. In Fig. 7, black area was the final detected liver region, from which we can see the two connected organ or tissues were successfully eliminated with a light gray color expressed. Figure 8 was the outlined liver contour described on the original image. We may notice that the contour was not fit the liver edge well, this is due to the thickening of edge on Fig. 6 (a) may decrease some liver information on the edge.

Error image in Fig. 9 (c) informs the error pixels $A_{err}$ with 502 points, and the liver area $A_{gold}$ is with 5121 pixels. Therefore, the error in this example was 9.8% (502/5121). Among these 502 pixels, majority error pixels were from liver edge, that implied the error ratio should be cut down by using additional re-detection step such as region growing to find out the lost edge information. Figure 13 illustrates the results of error rates for 30 MR images, in which some unsuccessful segmented examples are mainly with stomach strongly connecting to liver region, and the edges between them are not salient. However, it should be noted that our method tended to attenuate the connection after re-detection step. Some of these connectivity can be eliminated by us-

ing morphologic techniques if such connection is not strong. For example, shrinking the liver region and labeling iteratively till two labels are separated. However, we should lose some part of liver if the iterations are large.

In MR cases, the volume ratio LTW was relatively higher in cirrhosis (case2) with 24.0% than in the normal case (case1) with 14.8% as illustrated in Table 2, corresponding to the cases shown in Fig. 10 (b) and Fig. 10 (a), respectively. These two cases were constructed by extracted 2D liver regions from MR images with a slice interval of 5 mm. Figure 10 (c) shows a normal liver constructed from CT scans in case3 with a slice interval of 1.25 mm. The ratio of LTW also showed relatively higher in cirrhosis than in the normal case identical with the result from MR imaging. In our experience, LTW only changed slightly from a slice interval of 1.25 mm to 5 mm. Although MR images provide rich information for volumetric analysis of cirrhosis, CT is still meaningful to this study as not every patient who undergoes CT makes MR inspection. Other organs like abdominal aorta, ribs, and spine can be extracted by our same edge detection based method, which is shown with the liver in Fig. 10 (d).

By now the segmentation of two lobes is based on the inter-segmental line, that corresponding to a plane on a 3D image. Therefore, the LTW ratio may be changed slightly by different sleeping postures of a patient. Our program is trying to be able to extract some 3D reference objects such as the umbilical fissure of a liver so as to limit the error of LTW ratio only with the accuracy of the segmentation of 3D liver.

Although it is ideal to include shrunk segment IV (the quadrate lobe) [12] to the right lobe and enlarged segment I (the caudate lobe) to the left lobe to improve the ratio, the program is hard to extract these two segments accurately. Since the sum volume of them changes slightly and all of them are small in size compared with the whole liver region, we can ignore these changes and put them to the right hepatic lobe.

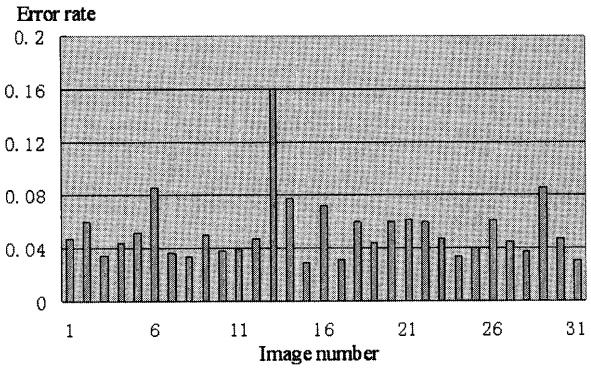


**Fig. 13** Error rates of segmentation on 30 MR cases.

Other potential usefulness of the 3D volume analysis program includes medical education, surgical planning, electronic clinical report and so on. In addition, our program can be extended to other organs like spleen, kidney or gallbladder. Since the volumes of spleen and gallbladder fossa are also very helpful sign of cirrhosis [13], [14], and the integration of such additional information into program would be our next goal of the current study.

We expect that the use of this LTW ratio will allow for more flexibility in evaluating the performance of volume analysis in predicting from early cirrhosis to advanced cirrhosis, but such a study requires a larger sample size of each disease state than does our current database contain.

In the future work, more images will be applied to test our segmentation algorithm, and the procedure of liver segment dividing by inter-segmental line and the selection of first image for segmentation should be automatic. Besides LTW ratio, texture analysis and shape analysis in the liver also may be helpful to differentiate cirrhosis according to our current study.

## 4. Conclusion

We have integrated an algorithm for 3D segmentation of liver region into volume calculation so as to estimate the degree of cirrhosis. The 3D liver is constructed by the hepatic contours extracted in every 2D slice. In order to determine the threshold value automatically, our method applies two edge detectors to obtaining the initial contour, from which the mean value is calculated as a reference for re-detecting step. The final contour is confirmed by thresholding technique. The result shows that the proposed method can robustly extract the liver region from MR and CT images. The total hepatic volume can be measured by our software automatically. From the result in Table 2, there is a weak correlation between cirrhosis and normal liver only with the whole hepatic volumes. However, by using the function of drawing the inter-segmental line, the radiologists can separate the 3D liver into two lobes manually, and the volume ratio of left-to-whole liver is expected to be useful in the

**Table 2** Results of LTW ratios in two MRI and two CT cases.

| Case No. | Image Type | Interval of slice | Clinical result | Whole volume ($mm^3$) | Left volume ($mm^3$) | LTW ratio |
|---|---|---|---|---|---|---|
| Case 1 | MRI | 5.0mm | Normal | 1037417 | 152959 | 14.8% |
| Case 2 | MRI | 5.0mm | Cirrhosis | 1113073 | 266560 | 24.0% |
| Case 3 | CT | 1.25mm | Normal | 1073408 | 167037 | 15.6% |
| Case 4 | CT | 1.25mm | Cirrhosis | 877311 | 237325 | 27.1% |

clinical examination of an in vivo hepatic radiographic image.

## Acknowledgments

Authors thank the members of Fujita Laboratory of Gifu University for their collaboration, especially to Tetsuji Tajima, who improved some algorithm on segmentation of liver. This research was supported in part by a research grant from the Collaborative Centre for Academy /Industry /Government of Gifu University, in part by the Ministry of Health, Labour, and Welfare under a Grant-In-Aid for Cancer Research and in part by the Ministry of Education, Culture, Sports, Science and Technology under a Grant-In-Aid for Scientific Research, Japanese Government.

### References

[1] K. Ito and D.G. Mitchell, "Hepatic morphologic changes in cirrhosis: MR imaging findings," Abdom. Imag., vol.25, pp.456–461, 2000.
[2] W.P. Harbin, N.J. Robert, and J.T. Ferrucci, "Diagnosis of cirrhosis based on regional changes in hepatic morphology: A radiological and pathological analysis," Radiology, vol.135, pp.273–283, 1980.
[3] W.E. Torres, L.F. Whitmire, and M.K. Gedgaudas, "Computed tomography of hepatic morphologic changes in cirrhosis of the liver," J. Comput. Assist. Tomogr., vol.11, pp.47–50, 1986.
[4] M. Zoli, D. Magalotti, M. Grimaldi, C. Gueli, G. Marchesini, and E. Pisi, "Physical examination of the liver: Is it still worth it?," Am. J. Gastroenterol, vol.90, pp.1428–1432, 1995.
[5] S. Bünyamin, E. Mehmet, U. Ahmet, I. Lütfi, B. Yüksel, B. Sait, and K. Süleyman, "Unbiased estimation of the liver volume by the Cavalieri principle using magnetic resonance images," Europ. J. of Radiol., vol.47, no.2, pp.164–170, 2003.
[6] C.R. McNeal, W.H. Maynard, R.A. Branch, T.A. Powers, P.A. Arns, K. Gunter, J.M. Fitzpatrick, and C.L. Partain, "Liver volume measurements and three-dimensional display from MR images," Radiology, vol.169, pp.851–864, 1988.
[7] H. Awaya, D. Mitchell, and T. Kamishima, "Cirrhosis: Modified caudate-right lobe ratio," Radiology, vol. 224, no.3, pp.769–774, 2002.
[8] K.Bae, M. Giger, and C. Chen, "Automatic segmentation of liver structure in CT images," Med. Phys., vol.20, no.1, pp.71–78, 1993.
[9] H. Park, P.H. Bland, and C.R. Meyer, "Construction of an abdominal probabilistic atlas and its application in segmentation," IEEE Trans. Med. Imaging, vol.22, no.4, pp.483–492, 2003.
[10] J. Masumoto, M. Hori, and Y. Sato, "Automated liver segmentation using multislice CT images," IEICE Trans. Inf. & Syst. (Japanese Edition), vol.J84-D-II, no.9, pp.2150–2161, Sept. 2001.
[11] D. Marr and E. Hildreth, "Theory of edge detection," Proc. Royal Society of London, B207, pp.187–217, 1980.
[12] M. Lafortune, L. Matricardi, and A. Denys, "Segment 4 (the quadrate lobe): A barometer of cirrhotic liver disease at US," Radiology, vol.206, pp.157–160, 1998.
[13] K. Ito, D.G. Mitchell, T. Gabata, and S.M. Hussain, "Expanded gallbladder fossa: Simple MR sign of cirrhosis," Radiology, vol.211, pp.723–726, 1999.
[14] K. Ito, D.G. Mitchell, and T. Gabata, "Enlargement of hilar periportal space: A sign of early cirrhosis at MR imaging," J. Magn. Reson. Imag., vol.11, pp.136–140, 2000.

**Xuejun Zhang** received the B.S. degree in Physics from Guangxi University, P.R.China, in 1991, and the M.S. degree in Electronics and Information Systems Engineering from Gifu University, Japan, in 2001. Currently, he is a Ph.D. candidate in Graduate School of Engineering from Gifu University, Japan. His research interests include artificial neural network, digital image processing and pattern recognition.

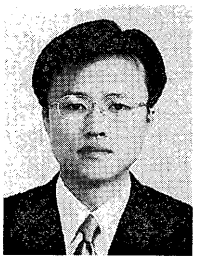

**Wenguang Li** received the B.S. degree in computer science from Harbin Institute of Technology, P.R.China, in 1997, and the M.S. degree in Electronics and Information Systems Engineering from Gifu University, Japan, in 2003. Since 2003, he has been with the Caravan Corporation. His research interests include image processing and network programming.

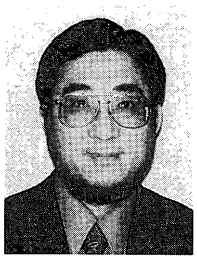

**Hiroshi Fujita** received the B.S. and M.S. degrees in Electrical Engineering from Gifu University, Japan, in 1976 and 1978, respectively, and Ph.D. degree from Nagoya University in 1983. He was a Research Associate at University of Chicago, USA, from 1983 to 1986. He is currently a Professor in the Department of Intelligent Image Information, Graduate School of Medicine, Gifu University, Japan. His research interests include computer-aided diagnosis system, image analysis and processing, and image evaluation in medicine.

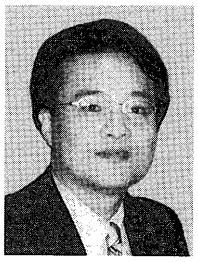

**Masayuki Kanematsu** (M.D.) received the Ph.D. degree at Gifu University in 1995. He served as a visiting scholar at Dept. of Radiology, University of Pittsburgh from 1994 to 1995. He has been appointed to the associated professorship of Radiology Services at Gifu University Hospital since 2001. He was invited as a visiting full professor of Dept. of Radiology, University of North Carolina from 2002 to 2003.

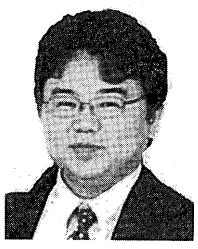

**Takeshi Hara** received the M.S. and Ph.D. degrees in Electrical Engineering from Gifu University, Japan, in 1995 and 2000, respectively. He is currently an associate professor in the Department of Intelligent Image Information, Graduate School of Medicine, Gifu University, Japan. His research interests include computer network, medical image processing and pattern recognition.

**Xiangrong Zhou** received the M.S. and Ph.D. degrees in information engineering from Nagoya University, Japan in 1997 and 2000 respectively. From 2000–2002, he continued his research in medical image processing as a postdoctoral researcher at Gifu University, and currently, he is a research associate of Graduate School of Medicine, Gifu University, Japan.

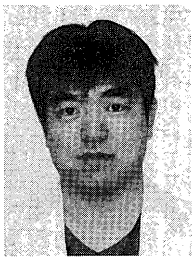

**Hiroshi Kondo** (M.D.) graduated from Gifu University School of Medicine in 1997. He is the Chief Radiologist of Department of Radiology, Kizawa Memorial Hospital, Minokamo, Japan. His specialty is abdominal radiology and interventions. He was awarded for his achievement in clinical radiologic research in 2002 by the Alumni Association of Gifu University School of Medicine.

**Hiroaki Hoshi** (M.D.) received the Ph.D. degree at Miyazaki Medical School in 1987. He served as a visiting scholar at the Montreal Neurological Institute from 1991 to 1992. He has been appointed to the chairmanship of Department of Radiology at Gifu University School of Medicine since 1995.